

Structure and Magnetic Switching of Thin-Film a-HITPERM/SiO₂ Soft Magnetic Multilayers

H. Okumura, C.-Y. Um, S.-Y. Chu, M. E. McHenry, D. E. Laughlin, and A. B. Kos

Abstract—Laminated (Fe_{0.7}Co_{0.3})₈₈Zr₇B₄Cu₁ amorphous HITPERM/SiO₂ multilayer thin films have been studied by room-temperature (RT) pulsed inductive microwave magnetometry (PIMM) in single, bilayer, and trilayer films. Switching has been measured in a multilayer film with six (50 nm) HITPERM layers, separated by five (2 nm) SiO₂ layers. Films were investigated by conventional transmission electron microscopy (TEM), high-resolution TEM (HREM), and superconducting quantum interference device (SQUID) magnetometry. HREM and TEM show BCC FeCo nanocrystals to nucleate on top of SiO₂ layers. Plan view TEM on the top layer reveals FCC nanocrystals that align in chains with spacing of ~50–100 nm. SQUID magnetometry shows reversal to begin by rotation in a single layer for $H < 14.4$ kA/m (180 Oe) followed by nearly simultaneous reversal of several layers. A final switching event is thermally activated, requiring fields in excess of 8 kA/m (100 Oe) to switch at 2 K, but switching at the same field as other layers for elevated temperatures (RT).

Index Terms—Multilayers, PIMM, soft magnet, thermally activated switching.

I. INTRODUCTION

THIN-FILM multilayers of the HITPERM composition (Fe_{0.7}Co_{0.3})₈₈Zr₇B₄Cu₁ are potential recording head materials [1], [2]. Zr-containing HITPERM has an induction of 1.7 T and Hf-containing HITPERM an induction of 2.0 T [3]–[5] with resistivities of 100–150 μΩ · cm. Magnetostriction coefficients of HITPERM melt-spun ribbons are $\lambda_s \sim 35$ ppm [6]. Laminating thin films and multilayers of amorphous HITPERM (a-HITPERM) separated by thin insulating SiO₂ interlayers limits the length scale over which eddy currents flow and allows structures with larger total magnetic moment. Nearly an order-of-magnitude reduction in the coercive field has been observed in nanolaminates as compared to single-layer films. We have previously demonstrated coercivities of less than 20 A/m (0.25 Oe) with film layer thicknesses of ~80 nm and SiO₂ thicknesses of 2.0–4.0 nm.

If eddy currents are restricted, the high frequency limit is governed by resonant absorption at the frequency of magnetization precession in the film. The resonant frequency is given by $\omega/\gamma \sim (4\pi MH_a)^{0.5}$ where the gyromagnetic factor,

$\gamma = -8.7941 \times 10^{10} \text{ s}^{-1}\text{T}^{-1}$ for orbital angular momentum, M , the magnetization, and H_a , the anisotropy field. High-frequency operation requires a large M and H_a (and switching by rotation). For a-HITPERM with saturation magnetization of ~1.5–1.7 T, and $H_a > 8$ kA/m (100 Oe) would result in a resonant frequency of several gigahertz. We have reported H_a s in bilayer and trilayer a-HITPERM of 2.8 kA/m (35 Oe) as measured by dc magnetization and FMR. Here, we report RT measurements of pulsed inductive microwave magnetometry (PIMM) in single, bilayer, and trilayer films.

We describe the switching in a multilayer film with 6 (50 nm thick) HITPERM layers, separated by 5 (2 nm thick) SiO₂ interlayers, where H_a 's as large as 14.4 kA/m (180 Oe) have been observed. We identify microstructural features thought to cause this large anisotropy field. As with prior observations on bilayer and trilayer films, we show thermally activated, stepped magnetization curves associated with sequential switching of layers [1], [2]. Potential implications of the stepped hysteresis on high-frequency switching will be discussed.

II. EXPERIMENTAL PROCEDURE

a-HITPERM thin films of single layers or multilayers were deposited on glass or Si (100) substrates using a Leybold–Heraeus Z400 rf sputtering system [7] with an Ar pressure of 1.33 Pa (10 mtorr), sputtering power density of 2.3 W/cm² and a substrate temperature of 24 °C. Cross-sectional transmission electron microscopy (TEM) samples were prepared by making a four-film sandwich on Si substrates, each glued together using epoxy and dried, followed by mechanical grinding and ion milling. For plan-view TEM samples, the ion milling process was performed only from the Si substrate side to observe the top layer(s) of the sputtered HITPERM film. JEOL JEM2000-EXII and Philips TECNAI-F20 TEMs [7] were used to study the film microstructures.

A Quantum Design superconducting quantum interference device (SQUID) magnetometer [7] was used to investigate switching by series of M – H hysteresis loops at temperatures of 2–60 K. The sample was first cooled from room temperature (RT) to 2 K in zero field and then saturated in an in-plane field of 24 kA/m (300 Oe). In a decreasing magnetic field, the hysteretic response at a given temperature was completely determined and the sample subsequently warmed in zero field and the same procedure repeated.

A PIMM [8] was used to measure the dynamic magnetization of the films. The PIMM uses a coplanar waveguide (CPW) structure to deliver high-speed (~100 ps rise time) field pulses causing the film's magnetization to rotate. The CPW structure is also used to inductively sense the sample magnetization as it precesses. Two measurements are taken: one with the sample

Manuscript received October 16, 2003. This work was supported by the National Institute of Standards and Technology (NIST) Magnetodynamics Program and the Carnegie Mellon University (CMU) Data Storage Systems Center.

H. Okumura (CMU) is with the Department of Socio-Environmental Energy Science, Kyoto University, Kyoto, Japan (e-mail: okumura@energy.kyoto-u.jp).

C.-Y. Um, S.-Y. Chu, M. E. McHenry, and D. E. Laughlin are with the Department of Materials Science and Engineering, Carnegie Mellon University, Pittsburgh, PA 15213 USA (e-mail: cyum@andrew.cmu.edu; sc79@andrew.cmu.edu; mm7g@andrew.cmu.edu; laughlin@cmu.edu).

A. B. Kos is with the National Institute of Standards and Technology, Boulder, CO 80305 USA (e-mail: kos@boulder.nist.gov).

Digital Object Identifier 10.1109/TMAG.2004.832109

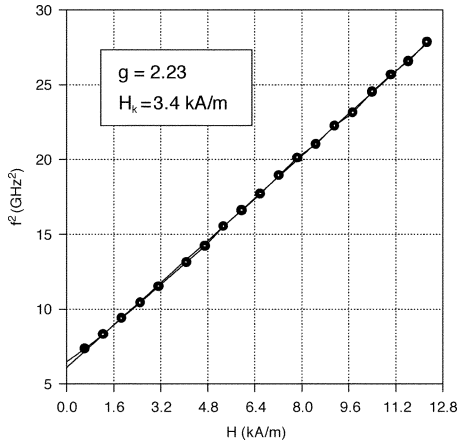


Fig. 1. PIMM results for 100 nm HITPERM sample showing linear fit of squared precessional frequency versus bias field. The Landé g -factor from the fit is 2.23 and the dynamic anisotropy field is 3.4 kA/m (43 Oe).

saturated by an external field applied in the same direction as the pulsed field, and a second with the sample allowed to rotate freely (no field). The two measurements are subtracted and integrated to yield a signal proportional to the sample magnetization. An external bias field, typically applied along the film's anisotropy axis, can be used to stiffen the response and increase the precessional frequency. These data can be used to calculate the Landé g -factor and H_a using standard ferromagnetic resonance (FMR) theory for fields parallel to the plane of the film [8].

III. RESULTS AND DISCUSSION

We begin by summarizing prior results along with new PIMM observations on single-layer films. For single-layer films, the coercivity is a minimum at a thickness of ~ 80 nm [1]. In a-HITPERM materials, with nonzero magnetostriction coefficients, a continuous transition between transverse and longitudinal stripe domains with decreasing film thickness [9] offers an explanation for the dependence of coercivity on film thickness. For single-layer films with thicknesses less than 100 nm, in-plane easy and hard axes were observed with $H_a = 2.8$ kA/m (35 Oe). Easy-axis hysteresis loops were square with a remanence ratio of ~ 0.98 . Prior results [2] showed the FMR frequency as a function of field to be fit by a Kittel equation with a single H_a . Fig. 1 shows the PIMM results of squared precessional frequency versus bias field and the associated fit for a 100-nm-thick HITPERM sample. Assuming $M_s = 1.45$ T, a straight line fit to the Kittel equation revealed a higher dynamic H_a (~ 3.4 kA/m) than measured statically (2.8 kA/m).

At thicknesses greater than 100 nm, no in-plane anisotropy was observed and the remanence ratio was ~ 0.7 and decreased in thicker films [1] (also a hallmark of dense stripe domains) [10]. A 150 nm single-layer film was studied by PIMM in this work. Here, the 150 nm film appeared isotropic and had to be initialized with an external field in the bias direction to allow even qualitative measurement with the PIMM. The PIMM delivers field pulses 200 A/m (2.5 Oe) in amplitude, which are large enough to allow measurement without disturbing this "temporary reset" in the 150 nm film.

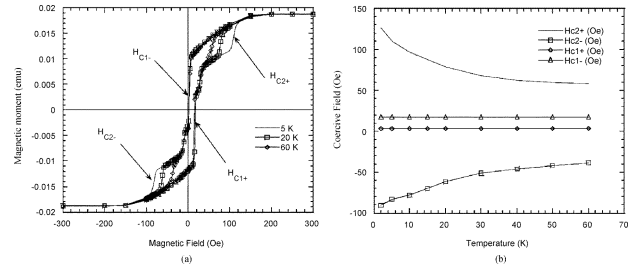


Fig. 2. (a) Magnetic dipole moment as a function of field for a six-layer laminated HITPERM film at $T = 5, 20,$ and 60 K, respectively and (b) the temperature dependence of the switching (coercive) fields H_{c1+} , H_{c1-} , H_{c2+} and H_{c2-} , respectively.

In double or bilayer films [11], a mechanism for this reduction in coercivity can be explained in terms of compensation of stray magnetic (wall) charges in one layer by corresponding structures in the other layer(s). Previously, we have observed coercivities approaching 80 A/m (1 Oe) to be achieved for single-layer a-HITPERM films with an order of magnitude reduction possible in multilayer films [1]. Larger damping coefficients were inferred from FMR linewidths [2] for bilayer and trilayer films as artifacts of slightly different anisotropy fields in the layers. Here, PIMM measurements on the same bilayer and trilayer films also exhibited large damping, but could not be fit with the Kittel equation, due to dispersion in anisotropy fields between layers.

Laminated HITPERM films have been shown to exhibit stepped magnetization curves with multiple states associated with sequential switching of various layers [1]. The switching is thermally activated, giving rise to higher coercivities at low temperature (< 40 – 100 K) than at RT. We have examined sequential switching in a multilayer film with six (50 nm) HITPERM layers, separated by five (2 nm) SiO₂ layers. Fig. 2 shows hysteric data for this film. For clarity, three typical field loops at $T = 5, 20, 60$ K are illustrated. Interesting observations include: (a) the loop is centered at $(H_{c1+} - H_{c1-})/2 \sim 800$ A/m (10 Oe) rather than zero field (consistent with an exchange bias effect). In comparison with the data of [1], we see that the magnitude of the field shift increases with the number of SiO₂ layers; and (b) after saturation, a strong rotational component of the switching is observed. The rotation of the magnetization in one layer about an anisotropy field of ~ 14.4 kA/m (180 Oe) is followed by nearly simultaneous switching of all but one remaining layer (a slight shoulder may indicate partial decoupling of this switching). Finally, thermally activated switching of the remaining layer is observed at H_{c2} . The T-dependence of the switching fields H_{c1+} , H_{c1-} , H_{c2+} and H_{c2-} are shown in Fig. 2(b). H_{c1+} and H_{c1-} are virtually independent of T. H_{c2+} and H_{c2-} are strongly T-dependent (roughly fit to a $H_{c2} = H_{c20}(1 - T/T_B)^{0.5}$).

Cross-sectional TEM studies of the six-layer HITPERM film (Fig. 3) showed each HITPERM layer to have a thickness of about 50 nm. Each layer is cleanly separated by ~ 2 nm SiO₂ layer with sharp interfaces with homogeneously distributed ultrafine embryos with sizes less than ~ 2 nm [2]. The top layer, however, contains larger nanocrystals with diameters of 10–20 nm. Both the larger and smaller nanocrystals have a BCC (B2) structure as determined by selected area diffraction (SAD) analyzes. Crystallites that appear larger than 20 nm are actually

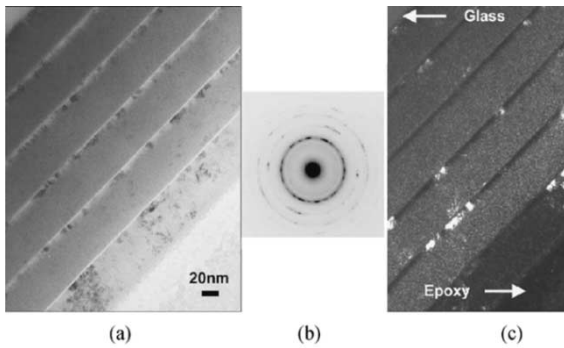


Fig. 3. Cross-sectional TEM on the top section of a six-layer laminated film showing nanocrystallization at the $\text{SiO}_2/\text{a-HITPERM}$ interface.

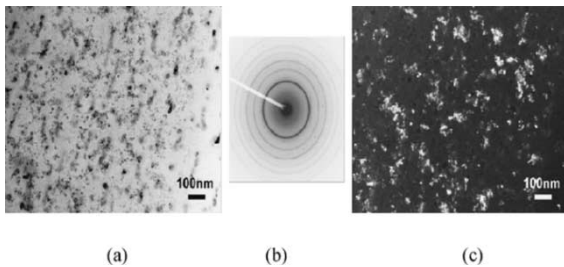


Fig. 4. Plan-view TEM on the top section of a six-layer laminated HITPERM film showing elongated FCC particles aligned in chains.

composed of many smaller clusters. Larger nanocrystallites form only on the top sides of SiO_2 layer. We attribute this preference to depletion of the Zr glass former which may react with the SiO_2 [2]. This indicates that Zr reactivity is a factor during the initial a-HITPERM layer deposition but not during the deposition of the SiO_2 layer over the top. The local depletion of Zr from the a-HITPERM lowers the activation barrier for nanocrystallization. The increased driving force for nucleation of nanocrystals drives the preferential nanocrystallization at the interface.

Nanocrystallization proceeds only to sizes of ~ 10 nm [4]. The orientation of the nanocrystals appears random and the random anisotropy model (RAM) still appears to be valid. However, nanocrystallization results in a local increase in the density and a consequent strain associated with contraction. This coupled to a magnetostriction coefficient of 36 ppm should give rise to magnetoelastic anisotropy which could be increased with a preferred alignment of the nanocrystals. Crystallographic texture (not observed) would lead to a break down in the RAM, while chains of nanoparticles would give rise to preferential directions for residual stress.

Plan-view TEM studies (bright field and dark field images) on the top two layers of the six-layered HITPERM film (Fig. 4) show the clustered nanocrystallites as described above in the cross-sectional TEM description. In addition, nanocrystal chains are observed. Elongated particle chains have lengths of ~ 100 – 200 nm, widths of 10 – 20 nm, and a spacing of 50 – 100 nm. Electron diffraction patterns exhibit rings corresponding to the BCC phase for the former clusters and dotted rings corresponding to the FCC phase for the elongated particles. The BCC phase has a lattice parameter of ~ 0.285 nm and the FCC phase has a lattice parameter of ~ 0.360 nm. Since the FeCo lattice parameter is $a = 0.2855$ nm, the BCC

phase is probably FeCo with some dissolved Zr and/or B atoms. The FCC phase has not been conclusively identified yet ($a = 0.3544$ nm for FCC Co and $a = 0.3589$ nm for FCC Fe, both measured at RT, suggests the γ -FeCo phase).

Observation of elongated (FCC) particles aligned in chains with a spacing of ~ 100 nm ($\sim 2 \times$ the HITPERM layer thickness) suggests that nanocrystallization may be aided by magnetoelastic interactions. Dense stripe domains are known to form with a periodicity related to the film thickness in very thin films [10]. Each subsequent layer in the multilayer film was deposited on a-HITPERM layers. The FCC nanocrystals may nucleate near strain free regions at walls between stripe domains where the barrier to nucleation is reduced. Chains define an easy magnetization direction due to magnetoelastic effects associated with contraction during nanocrystallization. Magnetoelastic interactions have a twofold effect: 1) reduced strain in the domain walls lowers the nucleation barrier and 2) nanocrystallization along the walls yields an anisotropic residual stress. The resulting induced anisotropy coupled with high magnetization may make these films potentially attractive for high-frequency applications. The thermally activated hysteresis suggests that losses may be a factor at elevated temperatures when driving the films at high frequency.

IV. CONCLUSION

Single, bilayer, and trilayer films of a-HITPERM/ $\text{SiO}_2(\text{Fe}_{0.7}\text{Co}_{0.3})_{88}\text{Zr}_7\text{B}_4\text{Cu}_1$ have been studied by PIMM and high f switching is qualitatively similar to previously reported FMR studies [2]. DC switching depends strongly on film thickness and whether the films are single or multilayer. Switching in a multilayer film with 6 (50 nm) a-HITPERM layers, separated by 5 (2 nm) SiO_2 layers showed a large H_a and a thermally activated switching. Plan view TEM on the top layer reveals FCC nanocrystals to align in chains with a spacing of ~ 100 nm. Alignment of nanocrystals in chains is postulated to occur due to a reduced barrier to nanocrystallization in strain-free regions at magnetostrictive stripe domain walls resulting in increased magnetic anisotropy.

REFERENCES

- [1] M. Q. Huang, Y. N. Hsu, M. E. McHenry, and D. E. Laughlin, *IEEE Trans. Magn.*, vol. 37, p. 2239, July 2001.
- [2] H. Okumura, D. J. Twisselmann, R. D. McMichael, M. Q. Huang, Y. N. Hsu, D. E. Laughlin, and M. E. McHenry, *J. Appl. Phys.*, vol. 93, no. 10, pp. 6528–6530, 2003.
- [3] M. A. Willard, D. E. Laughlin, and M. E. McHenry, *J. Appl. Phys.*, vol. 87, no. 9, p. 7091, 2000.
- [4] M. E. McHenry, M. A. Willard, and D. E. Laughlin, *Prog. Mat. Sci.*, vol. 44, p. 291, 2001.
- [5] F. Johnson, P. Hughes, R. Gallagher, D. E. Laughlin, M. E. McHenry, M. A. Willard, and V. G. Harris, *IEEE Trans. Magn.*, vol. 37, p. 2261, 2001.
- [6] F. Johnson, H. Garmestani, S. Y. Chu, H. Okumura, M. E. McHenry, and D. E. Laughlin, *J. Appl. Phys.*.
- [7] The identification of any commercial product or trade name does not imply endorsement or recommendation by the National Institute of Standards and Technology.
- [8] A. B. Kos, T. J. Silva, and P. Kabos, *Rev. Sci. Instrum.*, vol. 73, p. 3563, 2002.
- [9] R. W. Patterson and M. W. Muller, *Int. J. Magn.*, vol. 3, pp. 293–303, 1972.
- [10] A. Hubert and R. Schafer, *Magnetic Domains*. Berlin, Germany: Springer, 1998.
- [11] S. Middelhoek, *J. Appl. Phys.*, vol. 37, pp. 1276–1282, 1966.